23rd Int. Conf. Cyclotrons Appl. CYCLOTRONS2022, Beijing, China JACoW Publishing
ISBN: 978-3-95450-212-7 ISSN: 2673-5482 doi:10.18429/JACoW-CYCLOTRONS2022-FRA002

FEASIBILITY STUDY ON 10 MW-CLASS ULTRA-HIGH POWER CYCLOTRON

Tianjian Bian†, Shizhong An, Fengping Guan, Luyu Ji, Sumin Wei
China Institute of Atomic Energy, Beijing, China

Abstract

10 MW-class ultra-high power cyclotron (UHPC) has great application prospects in cutting-edge sciences, neutron source, advanced energy and advanced material, etc. So far, Cyclotron with average beam power of 10 MW still have some bottleneck problems. Beam energy and current of a high-power cyclotron are typically less than 800 MeV and 3 mA. In this paper, bottleneck problems of UHPC are analysed, and then a preliminary design of UHPC-10 MW is presented.

INTRODUCTION

GeV-class proton beam with an average power of several megawatts has many important applications in particle physics towards the intensity frontier, as well as in the advanced energy and material science. There are three different types of constructed accelerators for high power proton beam production: The cyclotron, linear accelerator and rapid-cycling synchrotron. The highest beam power of these accelerators currently is 1.4 MW. Reference [1] reported the energy efficiency of the three operational accelerators with the highest beam power in the world, which showed that the energy efficiency of the PSI cyclotron is about 2 times of the other types, as shown in Table 1. W. Weng made a judgement that the beam/grid efficiency should be better than 30%, otherwise the Accelerator Driven subcritical-reactor System (ADS) becomes nonsense [2]. Studies have shown that the energy efficiency cyclotron is the highest which is expected to be 60%~65% in superconducting ring cyclotron [3]. As cyclotron is a good technical route to develop proton machines with high beam power and high-power efficiency, it shows good prospect in advanced energy.

The beam power of UHPC-10 MW aims at 10 MW, it composes of two stages. The first stage is a 150 MeV/amu injector and the second stage is a 1 GeV/amu ring cyclotron. If UHPC-10 MW is used to drive a spallation neutron source, the injector and the ring cyclotron can produce thermal neutron flux in the order of 10^{14} n/cm^2/s and 10^{15}n/cm^2/s, respectively. UHPC-10 MW based spallation neutron source will have higher thermal neutron flux than high-flux reactor based neutron source. Even the 150MeV/amu injector can produce high thermal neutron flux which comparable to middle flux reactor neutron source. Figure 1 shows the history of thermal neutron flux [4], and UHPC-10 MW based spallation neutron sources are marked with stars.

* This work was supported by the National Natural Science Foundation of China (Grant No. 12105370) and the Scientific Research Program for Young Talent Elite Project of China National Nuclear Corporation (Grant No. FY212406000404).
† biantianjian@foxmail.com

Table 1: Efficiency of different types of high-power accelerators.

Accel-eator	Type	Energy (MeV)	Power (MW)	Effi-ciency
SNS	Linac	1000	1.3	8.6%
JPARC	synchro-tron	3000	1.0	3%
SINQ	cyclotron	590	1.4	18%

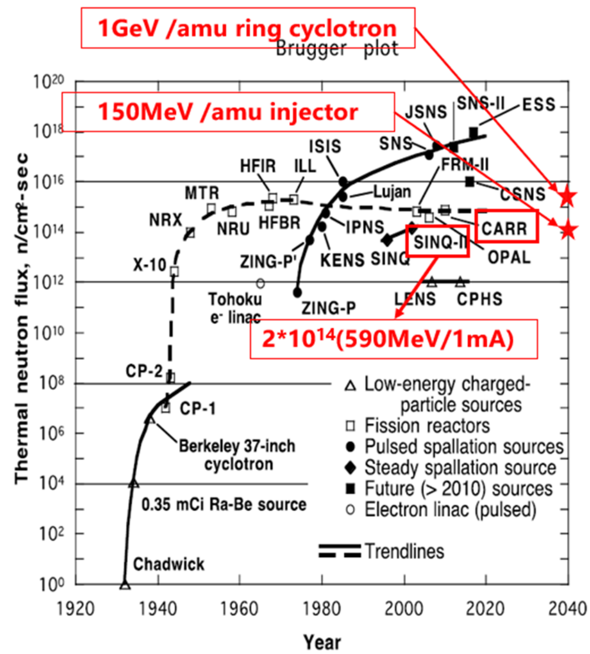

Figure 1: Thermal neutron flux history.

OVERALL DESIGN AND CONSIDERATION

Figure 2 shows the layout of UHPC-10MW. We choose a 1 MeV/amu RFQ as the pre-injector, and a separate sector cyclotron accelerate the beam from RFQ to 150 MeV/amu, finally the beam is injected to a 1 GeV/amu ring cyclotron.

Superconducting linac is the mainstream of high-power accelerator, due to relative higher technical maturity. So far, no well-approved design of 10 MW-class cyclotron is made due to some bottleneck problems. Radial tune is increasing linearly with beam energy in isochronous cyclotron, and thus the integer resonance crossing problem becomes an inevitable problem. Isochronous cyclotron is considered impossible to accelerate particles to a kinetic energy above its rest mass [5] typically 800 MeV/amu. Although cyclotron has continuous beam structure, the beam intensity is considered lower than 3 mA. The reason is enough clear region is need for beam extraction, otherwise the halo or tail particles will activate the deflector.

ISBN: 978-3-95450-212-7 ISSN: 2673-5482 doi:10.18429/JACoW-CYCLOTRONS2022-FRA002

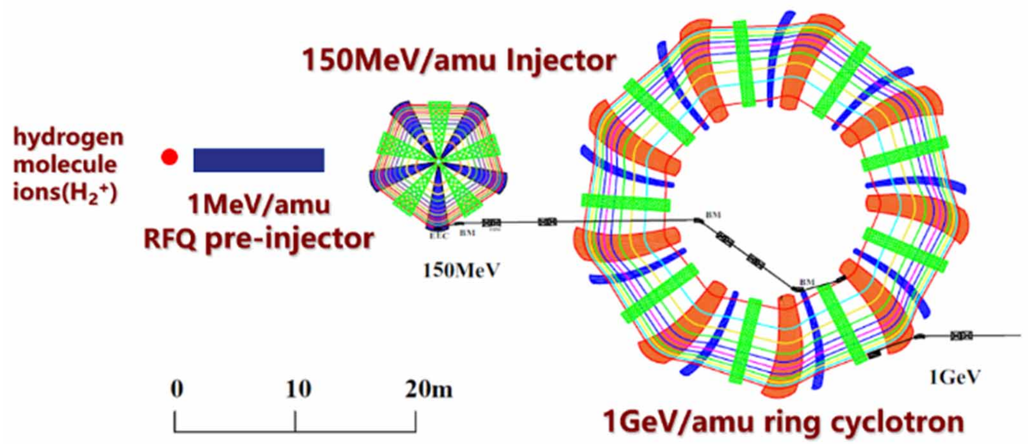

Figure 2: Layout of UHPC-10MW.

In the design phase of UHPC-10 MW, those problems need careful consideration and calculation. There are three bottleneck problems and their solutions:

(1) In low energy region, beam dynamics is dominated by space charge effect, so halo and tail particles are generated by space charge and non-adiabatic acceleration. In our design, we accelerate 5 mA of hydrogen molecule ions (H_2^+) instead of 10 mA of protons, which will mitigate the space charge effect [6].

(2) In high energy region, beam energy is limited by integer resonance. Beam integrates the harmonic field when passing through the integer resonance region, which drives large coherent oscillation. To solve those problems, an idea of integer resonance suppressor (IRS) was proposed [7]. IRS introduces the harmonic magnetic field intentionally to reduce the integration of driving harmonic field.

(3) In extraction region, single turn extraction with very low beam losses is also a very important issue of UHPC. The experience of PSI has shown that the upper limit of power deposition is 200 W. For 10 MW beam, relative losses should less than 2E-5. IRS can not only inhibit the radial oscillation and beam size blowup caused by integer resonance crossing but also contribute to a controllable coherent oscillation which is helpful to beam extraction with high efficiency [8]. With the help of IRS, turn separation can be enlarge to more than 30 mm.

150 MeV/amu INJECTOR

Parameters of 150 MeV/amu injector are listed in Table 2. 5 sectors scheme is adopted to avoid intrinsic resonance. Generous space between neighboring sectors can be used to install 5 powerful RF cavities. Beam is radially injected by a 1 MeV/amu RFQ pre-injector. Electrostatic deflector with a stripper foil placed upstream is used to high efficiency extraction.

To get the matched distribution, we track a coasting beam with 5 mA at 1 MeV/amu closed orbit until the equipartitioning process has resulted in a stationary distribution. Three cases with different phase width (9, 7, 6 rms degree) are simulated, as shown in Fig. 3. For those simulation, 10^4 particles and mesh of 32^3 grid points is used. In the coasting process, obvious longitudinal-radial coupling occurs and the gradually forms a round, compact distribution in 20 turns.

Table 2: Parameters of 150 MeV/amu Injector.

Parameter	Value
Accelerating particles	H2+
Extraction particles	H2+
Injection energy	1 MeV/amu
Extraction energy	150 MeV/amu
Extraction type	Electrostatic deflector
Turn separation at Extraction	~3 cm
Magnet sectors	5
Magnetic field of hill	3~3.7 T
Radius of pole	4.2 m
Cavity number	5
Harmonic number	7
Cavity frequency	~57 MHz
Cavity Voltage	~350 kV
Energy gain per turn	~3.4 MeV

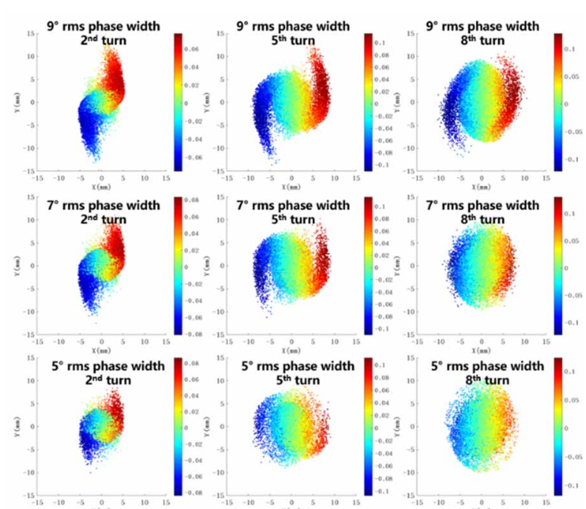

Figure 3: Longitudinal-radial coupling in the coasting process. Colour bars stand for energy deviation (MeV).

ISBN: 978-3-95450-212-7 ISSN: 2673-5482 doi:10.18429/JACoW-CYCLOTRONS2022-FRA002

Track the coasting beam for 50 turns and make statistics on beam parameters. Figure 4(a) and (b) show the relationship of beam parameters with phase width. We can find that both beam size and emittance are increasing with phase width. On the other hand, narrower phase width will develop into more compact distribution and wider phase width will lead to more halo particles, as shown in Fig. 4(c) and (d).

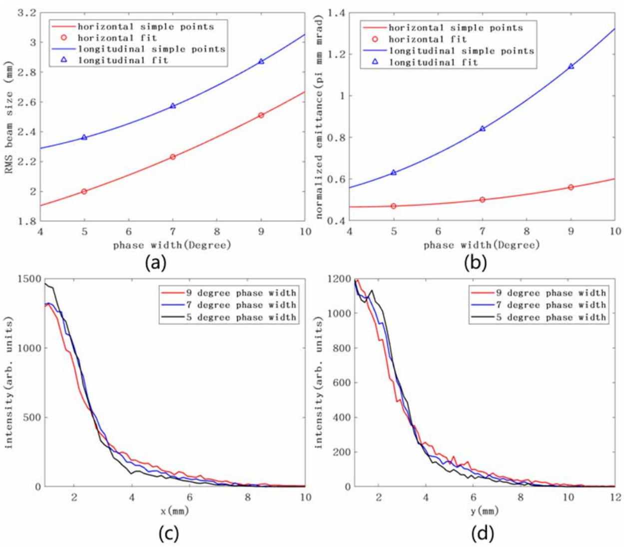

Figure 4: (a) Beam size as function of phase width. (b) Normalized emittance as function of phase width. (c) Distribution of matched beam in x direction. (d) Distribution of matched beam in y direction.

When acceleration is considered, beam halo will also increase due to nonadiabatic acceleration, especially in the low energy region. With contribution of acceleration and precession, turn separation is about 32 mm and the second and third to last turn overlap with each other. Beam is well controlled within ±6 mm in axial direction and septum is placed at the lowest intensity point, as shown in Fig. 5. If 0.5 mm is chosen as the septum thickness, the beam power at the deflector will be less than 30 W.

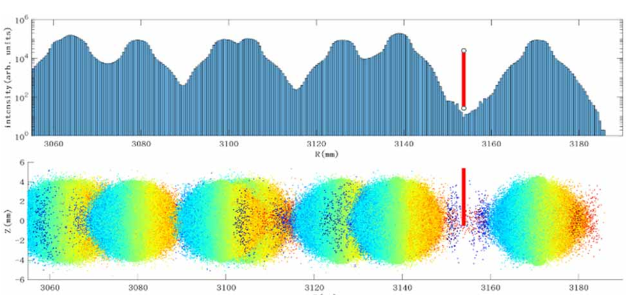

Figure 5: Beam intensity on radial probe.

1 GeV/amu RING CYCLOTRON

Parameters of 1 GeV/amu ring cyclotron are listed in Table 3. 9 high voltage RF cavities are installed in the space between neighboring sectors. Electrostatic deflector with a stripper foil placed upstream is used to high efficiency extraction.

Table 3: Parameters of 1 GeV/amu Injector

Parameter	Value
Accelerating particles	H2+
Extraction particles	H2+
Injection energy	150 MeV/amu
Extraction energy	1 GeV/amu
Extraction type	Electrostatic deflector
Turn separation at Extraction	~3cm
Cell number	9
Magnetic field of hill	2.7~4 T
Radius of pole	~11.2 m
Cavity number	9
Harmonic number	14
Cavity frequency	~57 MHz
Cavity Voltage	~1.3 MV
Energy gain per turn	~12 MeV
3^{rd} harmonic Cavity number	3
Voltage of 3^{rd} harmonic Cavity	10% of main cavity Voltage

In this ring cyclotron, beam is accelerated to beyond the integer resonance $\nu_r = 2$. In the extraction region, ν_r extend to nearly 2.5 to enlarge the turn separation. Figure 6 shows the tune diagram.

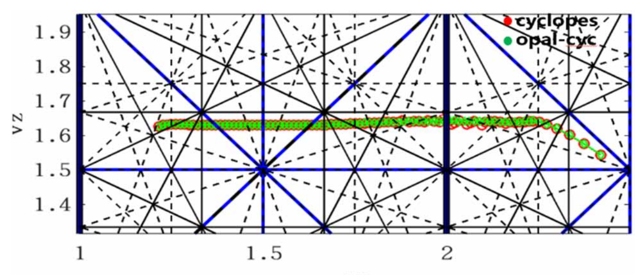

Figure 6: Tune diagram.

Beam integrates the harmonic field when passing through the integer resonance region, which drives large coherent oscillation. Second harmonic field B_2 of only 3Gs will drive coherent oscillation of 70 mm, which can be estimated with formula $\Delta A = \frac{\pi}{\sqrt{Q_\tau}} \frac{\bar{R}}{\bar{B}} \frac{B_2}{Q}$ [9]. Such large coherent oscillation is incompatible with the following resonance $4\nu_r = 9$ and the beam size is blown up. Figure 7(a) Shows that the radial beam size is increased about 2 times. One of the reasons is that intrinsic resonance $4\nu r = 9$ distorts the phase space, as shown in Fig. 7(b). IRS method is adopted to correct the large coherent motion before reaching the intrinsic resonance $4\nu_r = 9$. Figure 8 shows the structure and location of IRSs in the ring cyclotron. Coil current of IRSs marked by triangle and circle are oppositely directed. Coil current of IRSs marked by same colour have the same current value. Detailed structure and arrangement principle are explained in Ref. [7]. With the IRSs, radial oscillation is reduced to ±10 mm and the beam size is beam size will not be blown up, as shown in Fig. 9.

ISBN: 978-3-95450-212-7 ISSN: 2673-5482 doi:10.18429/JACoW-CYCLOTRONS2022-FRA002

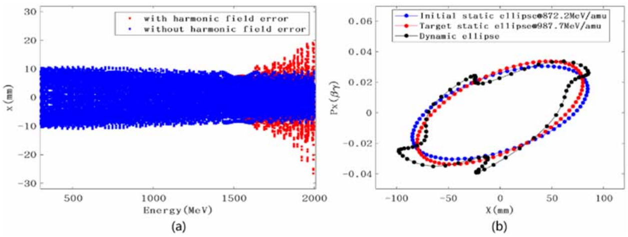

Figure 7: (a) Beam size evolution in the acceleration process. (b) Intrinsic resonance $4\nu r = 9$ distorts the phase space.

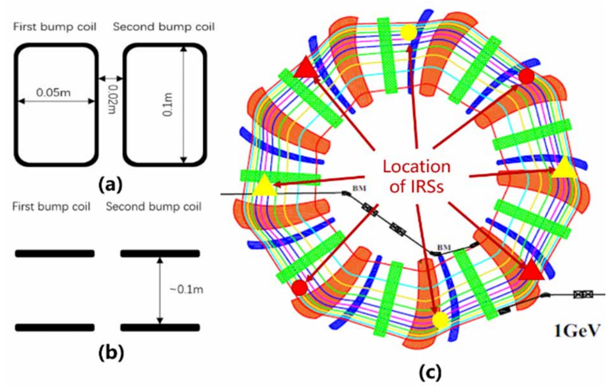

Figure 8: (a) Top view of an IRS. (b) Side view of an IRS. (c) Location of IRS in the ring cyclotron.

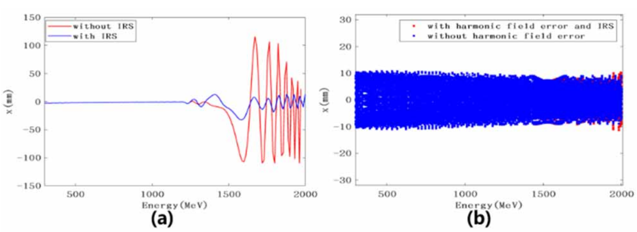

Figure 9: (a) Radial oscillation with and without IRS. (b) Beam size evolution with and without IRS.

With contribution of acceleration and precession, turn separation is about 35 mm. The space charge effect also has powerful influence on the beam dynamics. Figure 10 shows beam intensity on radial probe for different phase width. The emittance is 1 π mm rad and $25 \cdot 10^4$ macro particles and mesh of 32^3 grid points is used. For 2°rms phase width, space charge dominates the beam dynamics. A round, compact beam is developed due to vortex motion, but the beam will break up in the integer resonance crossing process. For 8°rms phase width, beam dynamics is dominated by emittance and the turn separation is much more clear. The case with 5°rms phase width is at the trans ition between the emittance-dominated and space- charge-dominated. For the optimized case, 7.5°rms phase width and 2.5 π mm rad is used and then a clear region is obtained at the extraction point. If 0.5 mm is chosen as the septum thickness, the beam power at the deflector will be less than 100 W.

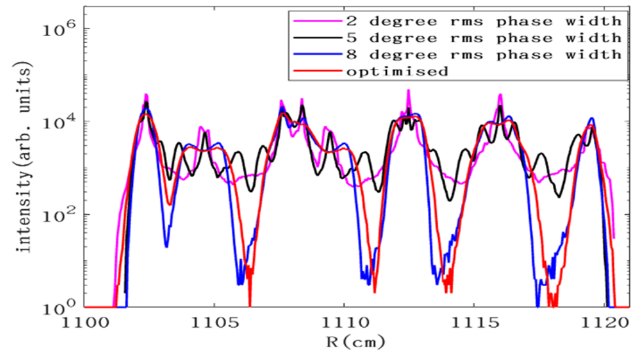

Figure 10: Beam intensity on radial probe for different phase width.

SUMMARY

This paper presents the preliminary design of UHPC-10 MW. Simulation results of beam power deposition on deflector show that the margin is sufficient. In particular, the 1 GeV/amu ring cyclotron accelerate the beam to beyond the integer resonance and IRS is used to control the oscillation. Simulations show that IRS can not only reduce the beam size growth rate to less than 5%, but also enlarge the turn separation to 35mm. That is to say, IRS not only acts as integer resonance suppressor, but also plays the role of separation optimizer between the last and second last turn. From our limited knowledge, we do not see any fundamental limits that prevent the construction of a 10MW-class cyclotron. OPAL [10] and Cyclops [11] are used in the beam dynamics simulation.

REFERENCE

[1] J. Grillenberger, M. Seidel, S.-H. Kim, M. Yoshii, and V. P. Yakovlev, "The energy efficiency of high intensity proton driver concepts", in *Proc. IPAC'17*, Copenhagen, Denmark, May 2017, pp. 4842-4847. `doi:10.18429/JACoW-IPAC2017-FRXCB1`

[2] W. Weng, "Developments of High Power Proton Accelerators", Brookhaven National Lab., Upton, NY, USA, 2018, unpublished

[3] L. Calabretta et al., "Cyclotrons and FFAG accelerators as drivers for ADS*", Rev. Accel. Sci. Technol.*, vol. 08, pp. 77-97, 2015.

[4] J. M. Carpenter, "Accelerator-based neutron sources: past, present, and future", Oct. 2018, unpublished, `http://flnph.jinr.ru/images/content/Carpenter.pdf`

[5] L. A. Sarkisyan, "Possibility of accelerating protons to energies above E0 in an isochronous cyclotron", Soviet Atomic Energy, vol. 30, pp. 584–586, 1971.

[6] J. Alonso *et al.*, "The IsoDAR High Intensity H2+ Transport and Injection Tests", *J. Instrum*., vol. 10, p. T10003, 2015. `doi:10.1088/1748-0221/10/10/T10003`

[7] T. Bian *et al.,* "Possible solution for the integer resonance crossing problem of GeV-class isochronous Fixed-Field Alternating Gradient accelerators", *Nucl. Instrum. Methods Phys. Res. Sect. A*, vol. 1031, p. 166594, 2022. `doi:10.1016/j.nima.2022.166594`

ISBN: 978-3-95450-212-7 ISSN: 2673-5482 doi:10.18429/JACoW-CYCLOTRONS2022-FRA002

[8] T. Bian *et al.,* "Inhibition and Utilization of Integer Resonance in GeV/mA Class High Power Circular Accelerator", *Atomic Energy Science and Technology*, 2022, vol. 9, p. 056, 2022, in Chinese.

[9] R. Baartman, "Fast crossing of betatron resonances", presented at the FFAG Workshop, TRIUMF, Vancouver, BC, Canada, Apr. 2004, https://ffag2004.triumf.ca/

[10] M. M. Gordon, "Computation of closed orbits and basic focusing properties for sector-focused cyclotrons and the design of 'cyclops'", *Part. Accel.*, vol. 16, pp. 39-62,1984.

[11] Object Oriented Parallel Accelerator Library (OPAL), https://gitlab.psi.ch/OPAL/src/-/wikis/home